DEVELOPMENTAL DYNAMICS 237:1334–1347, 2008

RESEARCH ARTICLE

Hsp60C Is Required in Follicle as Well as Germline Cells During Oogenesis in *Drosophila melanogaster*

Surajit Sarkar[†] and S.C. Lakhotia[*]

Hsp60C* gene of *Drosophila melanogaster* shows a dynamic spatiotemporal expression during oogenesis and seems to contribute bulk of the Hsp60 family proteins in ovarioles. Hsp60 distribution overlaps with that of F-actin–rich membranes/structures in follicle, nurse, and egg cells throughout oogenesis. Skeletal muscle fibers associated with ovarioles and in other parts of the body show patterned location of Hsp60 in A-bands. During stages 11–12, Hsp60 accumulates at junctions of nurse cells and oocyte, where a new microtubule organizing center is known to develop. A recessive hypomorph allele, *Hsp60C^{1}* causes complete sterility of the rare surviving homozygous adults. Their egg chambers show very little Hsp60C transcripts or Hsp60 protein. Beginning at stages 6–7, *Hsp60C^{1}* chambers show a disorganized follicle cell layer with poor cell adhesion in addition to abnormal organization of F-actin and other cytoskeletal structures in follicle, nurse, and egg cells. Additionally, expression and localizations of Hrb98DE, Squid, and Gurken proteins in nurse cells and oocyte are also severely affected. *Hsp60C^{1}* homozygous follicle cell clones in *Hsp60C^{1}*/+ ovarioles show disruptions in follicle epithelial and cytoskeleton arrangements. Likewise, egg chambers with *Hsp60C^{1}* homozygous germline clones in *Hsp60C^{1}*/+ flies show abnormal oogenesis. Our results provide the first evidence for an essential role of Hsp60C in *Drosophila* oogenesis, especially in organization and maintenance of cytoskeletal and cell adhesion components. *Developmental Dynamics 237:1334–1347, 2008. © 2008 Wiley-Liss, Inc.

Key words: follicle cells; actin, MTOC; cell adhesion; cytoskeleton; striated muscles

Accepted 23 February 2008

INTRODUCTION

The Hsp60 or chaperonin family is a highly conserved group of molecular chaperones and includes bacterial GroEL, mitochondrial Hsp60, plastid Rubisco subunit binding protein, archaea group II chaperonins, eukaryotic cytosolic Tcp-1 protein, and so on, and are most well known for their organelle localization and roles in protein folding (Ranson et al., 1998; Hartl and Hayer-Hartl, 2002). In recent years, however, they have also been found to be involved in a variety of nonchaperonic functions such as cell signaling, epithelial cell remodeling/motility, apoptosis, and so on (Maguire et al., 2002; Gobert et al., 2004; Zhang et al., 2004; Sarkar et al., 2006; Arya et al., 2007). Besides being present in the organelles (mitochondria or chloroplasts), the Hsp60 proteins are now known to be present in cytosol, on cell membrane or even outside the cell (Maguire et al., 2002; Sarkar et al., 2006).

Four Hsp60-like DNA sequences have been reported in *Drosophila melanogaster* (www.flybase.org), which on the basis of their putative protein products are classified as members of the *Hsp60* gene family and named, respectively, as *Hsp60A* at 10A4 polytene band, *Hsp60B* at 21D2 band, *Hsp60C* at 25F2 band and *Hsp60D* at 34C1 band (Sarkar and Lakhotia, 2005). As expected (Betran et al., 2002), these duplicated genes have acquired distinct functions (Sarkar and

Cytogenetics Laboratory, Department of Zoology, Banaras Hindu University, Varanasi, India
[†]Dr. Sarkar's present address is Department of Genetics, University of Delhi, South Campus, New Delhi 110 021, India.
[*]Correspondence to: S.C. Lakhotia, Cytogenetics Laboratory, Department of Zoology, Banaras Hindu University, Varanasi 221 005, India. E-mail: lakhotia@bhu.ac.in

DOI 10.1002/dvdy.21524
Published online 3 April 2008 in Wiley InterScience (www.interscience.wiley.com).

Lakhotia, 2005). While the *Hsp60A* gene seems to be the ubiquitously expressed general chaperonin (Perezgasga et al., 1999), *Hsp60B* has testis-specific expression and is essential for sperm individualization (Timakov and Zhang, 2001). The *Hsp60C* gene has been shown to be required for tracheal development and for early stages in spermatogenesis (Sarkar and Lakhotia, 2005), and one of the roles of the *Hsp60D* gene seems to be in modulation of apoptosis (Arya et al., 2007).

In an earlier report, we (Sarkar and Lakhotia, 2005) described a new $Hsp60C^1$ allele, which carries a P-transposon in the promoter region of the *Hsp60C* gene and thus affects its expression. Homozygosity for this strongly hypomorphic $Hsp60C^1$ allele results in tracheal defects and early first instar larval lethality. Interestingly, ~10% of the $Hsp60C^1$ homozygotes survive as weak and completely sterile adults. In our previous study (Sarkar and Lakhotia, 2005), we examined spermatogenesis in the rare surviving $Hsp60C^1$ homozygous adult flies and found that, unlike the requirement of the *Hsp60B* gene for individualization of sperms (Timakov and Zhang, 2001), the $Hsp60C^1$ mutant allele affects early stages of spermatogenesis. In the present study, we examined expression of *Hsp60C* gene during oogenesis and the basis for complete sterility of surviving $Hsp60C^1$ homozygous females.

Oogenesis in *Drosophila* is a complex developmental process involving extensive cellular remodeling events and complex intercellular communications. Development of egg chamber has been subdivided into a series of 14 consecutive stages characterized by distinct morphological criteria (King, 1970). A monolayer of somatic follicle cells covers the 16 germline-derived cells (15 nurse cells and 1 oocyte) in each egg chamber. Nurse cells and the oocyte remain interconnected by means of a stereotyped pattern of F-actin–based ring canals (King, 1970; Spradling, 1993). An intricate orchestration of DE-cadherin– and β-catenin–dependent adhesion between oocyte and follicle cells, the actin- and tubulin-based cytoskeletal elements and appropriate signaling between the different cell types in egg chamber is critical for progression of oogenesis and production of a functional egg (Peifer et al., 1993; Gonzalez-Reyes and St Johnston, 1998; Wodarz, 2002).

Our results show that the Hsp60C transcripts are abundant in egg chambers and the Hsp60C protein is a major component of Hsp60 family proteins in these cells. Hsp60 and F-actin show a significant overlap/association in follicle and nurse cells and in the cortex of early/mid stage oocytes. Furthermore, a remarkable concentration of Hsp60 is seen in basal nurse cells and at the anterior oocyte cortex in stage 11–12 wild-type chambers, in the region where the bicoid transcripts are known to be localized in the oocyte cytoplasm and where a microtubule organizing center (MTOC) forms during these stages (Schnorrer et al., 2002). The $Hsp60C^1$ mutants' egg chambers show little Hsp60 at any of these sites, while the cytoskeletal elements (e.g., cell adhesion molecules, F-actin, tubulin, etc.) in all cell types are severely affected. Hsp60 also shows a remarkable localization in the A-bands of skeletal muscles, including those surrounding the egg chambers and the ovarioles in wild-type but not in the $Hsp60C^1$ mutant flies. Analysis of $Hsp60C^1$ homozygous mutant cell clones in $Hsp60C^1$/+ egg chambers confirmed the essential requirement of Hsp60C for follicle layer organization. Likewise, the $Hsp60C^1$ homozygous germline clones in $Hsp60C^1$/+ flies show abnormal cytoskeleton and other abnormalities. It appears that in addition to the earlier noted (Sarkar and Lakhotia, 2005) role of the Hsp60C protein in tracheal development and spermatogenesis, this protein is also essential for skeletal muscle organization and oogenesis in *Drosophila*.

RESULTS

$Hsp60C^1$ Homozygous Females Are Sterile

Ovaries of all surviving $Hsp60C^1$/$Hsp60C^1$ adult females were much smaller than in wild-type due to near absence of late stage follicles, with most ovarioles showing degenerated material at their distal ends. The numbers of ovarioles per ovary (N = 28) was, however, not affected. Other female reproductive organs in

Fig. 1. A–D: Phase contrast images of a laid wild-type egg (A) and defective eggs recovered from oviducts of $Hsp60C^1$/$Hsp60C^1$ females (B–D) that show patterning defects and abnormally located (B) or poorly developed (C) dorsal appendages. The egg in D looks like a stage 13 egg chamber exhibiting a "dumpless" phenotype. Scale bar = 100 μm.

$Hsp60C^1$ mutant flies appeared generally comparable to those in wild-type (not shown). The $Hsp60C^1$/$Hsp60C^1$ females never laid any eggs, although a few abnormal and collapsed eggs with patterning defects could be recovered from the oviduct (Fig. 1). Compared with wild-type (Fig. 1A), these eggs were fragile and the majority of them showed poorly developed and improperly oriented dorsal appendages (Fig. 1B), while a few were without them (Fig. 1C,D). In addition, some eggs with incomplete dumping (Fig. 1D) were also seen.

The viability as well as fertility of $Hsp60C^1$/$Hsp60C^1$ females was restored in the P-transposon excision lines (Sarkar and Lakhotia, 2005). Defects in oogenesis in $Hsp60C^1$/*Df(2L)cl-h2* females were similar to those in $Hsp60C^1$/$Hsp60C^1$ females (see Table 1). Thus, the $Hsp60C^1$ is a loss of function mutation and is responsible for complete sterility of the few surviving $Hsp60C^1$ homozygous adult females.

Hsp60C Gene Is Expressed in a Stage-Specific Pattern During Oogenesis

The Hsp60C transcripts in reproductive organs of adult wild-type female flies were localized by RNA:RNA in situ hybridization with *Hsp60C*-specific riboprobe (Sarkar and Lakhotia, 2005). In female reproductive organs of wild-type flies, a strong expression of *Hsp60C* was seen in the ovarioles and spermathecae but little in calyx, oviduct, seminal re-

TABLE 1. Stage 7 and Later Egg Chambers of *Hsp60C[1]* Mutant Flies Show a Variety of Abnormalities

Genotype	N	Normal egg chambers	Degenerating egg chambers[a]	Misplaced oocyte[a]	Binucleate/ multinucleate nurse cells[a]	Multiple defects[a]
+/+	136	92.0%	2.2%	1.0%	1.5%	2.2%
Hsp60C[1]/+	136	84.5%	2.2%	1.5%	2.2%	4.5%
Hsp60C[1]/*Hsp60C[1]*	94	Nil	25.5%	8.5%	6.5%	25.5%
Hsp60C[1]/*Df(2L)cl-h2*	86	Nil	25.0%	13.0%	1.5%	32.5%

[a] The follicle cell layer in all of these egg chambers was affected.

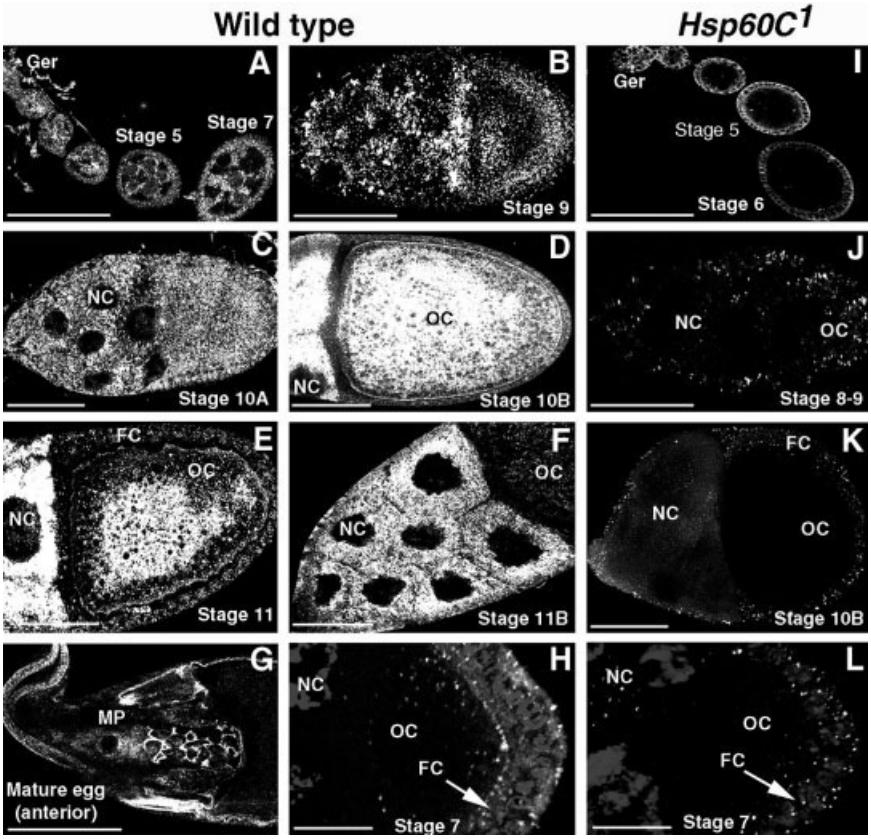

Fig. 2. A–L: Confocal optical sections of wild-type (A–H) and *Hsp60C[1]*/*Hsp60C[1]* (I–L) egg chambers after in situ hybridization to cellular Hsp60C transcripts (bright fluorescence). The egg chamber stages are marked in each panel. H and L are high-magnification images of posterior follicle cells in sectional view from wild-type (H) and *Hsp60C[1]*/*Hsp60C[1]* (L) stage 7 egg chambers to show the highly reduced levels of Hsp60C transcripts in cytoplasm of mutant follicle cells and the absence of regular intercellular tight association between them (4′,6-Diamino-2-phenylindole dihydrochloride [DAPI] stained nuclei appear gray in H and L). Ger, germarium; MP, micropyle region; NC, Nurse cells; OC, oocyte; FC, Follicle cell. Scale bars = 50 μm in A–G,I–K, 5 μm in H,L.

ceptacles, accessory glands, and the genital chamber (not shown).

Confocal microscopic examination of distribution of Hsp60C transcripts in developing wild-type egg chambers (Fig. 2) revealed the transcripts to be mostly present in cytoplasm of follicle and nurse cells. The level of Hsp60C transcripts was low in the germarium and in follicle and nurse cells of early stage egg chambers (Fig. 2A,B). Of interest, while the follicle cells continued to show a similar low level of hybridization until stage 12 of oogenesis, nurse cells and the growing oocyte showed a dynamic pattern. Level of Hsp60C transcripts in nurse cells and in oocyte increased until stage 10B (Fig. 2B–F), after which, a decline was seen first in the oocyte (Fig. 2E,F) followed by nurse cells. Mature oocyte had little of Hsp60C transcripts (Fig. 2G), although some localized hybridization signal was seen in region where the future micropyle would develop (Fig. 2G).

To determine the distribution of Hsp60 protein, we stained egg chambers with anti-Hsp60 antibody SPA 805 (StressGen, Canada), which is believed to detect all the four Hsp60 forms present in *D. melanogaster* (Lakhotia et al., 2002). These preparations were counterstained with tetrarhodamine isothiocyanate (TRITC) -Phalloidin and 4′,6-diamino-2-phenylindole dihydrochloride (DAPI) to detect F-actin and DNA, respectively.

Hsp60 was specifically localized in the myosin-rich A-bands of striated muscles that wrap each ovariole (not shown) and individual egg chambers (Fig. 3A) of wild-type flies. A comparable specific localization of Hsp60 in A-bands was seen in striated muscles of oviduct wall (Fig. 3B) and in other parts of body (not shown).

Follicle cells in wild-type egg chambers showed abundant presence of Hsp60 in their cytoplasm. Hsp60 and F-actin overlapped along cell membranes between adjacent follicle cells (Fig. 3C–C″). Confocal images of lateral views of follicle cells, however, revealed a higher concentration of Hsp60 on the external face of follicle cells while F-actin was more abundant on the internal face opposing nurse cells and oocyte (Fig. 3D–D″).

Confocal images of inner optical sections of wild-type egg chambers revealed an interesting pattern of distribution of Hsp60 at different stages of oogenesis (Fig. 3E–H). Hsp60 was present in nurse cell cytoplasm with enhanced concentration near cell

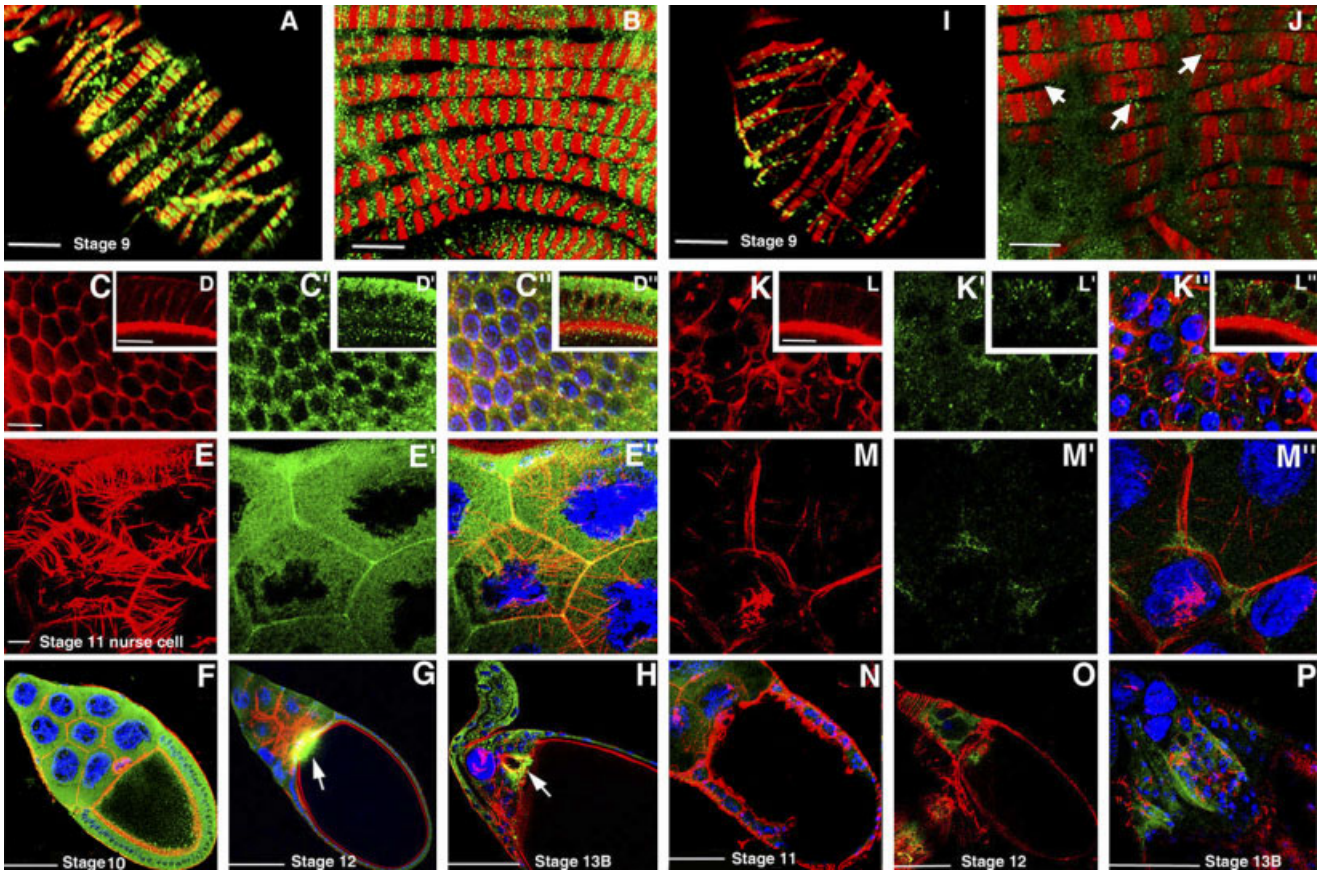

Fig. 3. A–P: Confocal images to show localization of F-actin (red, A–P) and Hsp60 (green, A–C′,D′,E′,F–K′,L′,M′,N–P) in striated muscles surrounding a stage 9 egg chamber (A,I), oviduct muscles (B,J), and in follicle cells (C–C″,D–D″,K–K″,L–L″), nurse cells and oocyte (E–E″,F–H, M–M″,N–P) in wild-type (A–H) and *Hsp60C*^{1}/*Hsp60C*^{1} (I–P) egg chambers. A–C″,D″,E″,F–K″,L″,M″,N–P show merged images. Lateral views of follicle cells are shown at higher magnification in D–D″ and L–L″. Arrows in J indicate disruptions in lateral register of actomyosin fibrils in a muscle bundle. Arrow in G shows the increased concentration of Hsp60 and F-actin at the junction of basal nurse cells and the anterior region of the oocyte during stages 11–12, where the anterior microtubule organizing center (MTOC) is believed to be formed (Schnorrer et al., 2002). Arrow in H marks the future micropyle region where Hsp60 gets restricted beginning with stage 13B. The mutant egg chambers (N–P) show disorganized F-actin cytoskeletal elements and very little Hsp60. Scale bars = 5 μm in A,C–E″,I,K–M″, 10 μm in B,J, 50 μm in F–H,N–P.

membrane (Fig. 3E–E″). Its level increased in nurse cells from early to stage 10 chambers and its cellular distribution overlapped with that of F-actin, particularly at cell membranes. Hsp60 was also seen to cover the cables of actin scaffold that develop around the large polyploid nuclei in nurse cells (Hudson and Cooley, 2002). Compared with nurse and follicle cells, the growing oocyte showed less Hsp60 and F-actin, both of which, until stage 10B, were overlappingly concentrated along the cell membrane and cortical layer. Hsp60 also spread a little further into the oocyte cytoplasm (Fig. 3F). In later egg chambers (Fig. 3G,H), in parallel with the distribution of Hsp60C transcripts (Fig. 2), Hsp60 became increasingly less abundant in most nurse cells and the oocyte, while the follicle cells continued to show moderate levels of Hsp60 along with F-actin near cell membranes. Beginning with stage 10B and continuing until early stage 13, when most of the nurse cells showed reduction in cytoplasmic Hsp60, an increase in concentration of Hsp60, and of F-actin, was detected at the basal nurse cell cytoplasm near the anterior margin of oocyte (Fig. 3F,G). Interestingly, F-actin was absent in the anterior oocyte cytoplasm where Hsp60 was concentrated during stages 10–12 (Fig. 3F,G). Location of the redistributed Hsp60 at stage 10B is in the area where γ-tubulin is reported to be localized at the beginning of stage 10B for development of a distinct MTOC (Schnorrer et al., 2002). In other parts of the oocyte, Hsp60 disappeared almost completely, although F-actin continued to be present cortically (Fig. 3G,H). Following stage 13, Hsp60 completely disappeared from the anterior oocyte cytoplasm while on the nurse cell face, it remained confined to a small area near the nurse cell–oocyte junction, which would subsequently form the micropyle (Fig. 3H). During stage 13, Hsp60 was seen exclusively surrounding the future micropyle area along with F-actin, but in more mature egg chambers, F-actin disappeared from this region while Hsp60 was still present (not shown).

Hsp60C^{1} Mutant Egg Chambers Show Little Hsp60C Transcripts and Hsp60 Protein

Ovaries from *Hsp60C*^{1} homozygous females showed very little hybridization with the Hsp60C riboprobe. In intact

ovaries, some detectable signal was seen in the associated tracheoles, but this was significantly less than in wild-type ovaries (not shown). Spermathecae also showed little hybridization (not shown). The significantly reduced levels of *Hsp60C* transcripts in the mutant ovaries and spermathecae further confirm that the *Hsp60C^{1}* is a severe hypomorphic allele (Sarkar and Lakhotia, 2005).

Confocal microscopy confirmed substantially reduced levels of Hsp60C transcripts in egg chambers from *Hsp60C^{1}* homozygous flies (Fig. 2I–L). The germline cells showed little Hsp60C transcripts in the very early stages (Fig. 2I–K). During later stages, while nurse cells occasionally displayed low levels of transcripts (Fig. 2J,K), little hybridization was detected in the oocyte at any stage (Fig. 2J–L). The level of Hsp60C transcripts in follicle cells until stage 4–5 in the mutant ovaries was less severely affected (compare Fig. 2A with 2I), but in later mutant egg chambers, the follicle cells also showed significantly reduced levels of Hsp60C transcripts. As seen in higher magnification images of follicle cells (Fig. 2H,L), compared with the large and many clusters of Hsp60C transcripts in wild-type follicle cells (Fig. 2H), the mutant follicle cells displayed smaller and fewer clusters (Fig. 2L).

The muscle layers surrounding ovarioles, individual egg chambers (Fig. 3I), and oviduct wall (Fig. 3J) in *Hsp60C^{1}* homozygous flies showed significantly less Hsp60 in the myosin-rich A-bands. F-actin staining revealed that the bundles of muscle fiber in the mutant ovarioles were irregular and thinner than those in wild-type with component fibrils of bundle often not in register (compare Figs. 3A,B and 3I,J).

The germarium and early stage egg chambers of *Hsp60C^{1}* mutant flies showed very little Hsp60 in follicle or nurse cells (Fig. 3K–M″) with weak signals seen at some places near the outer membranes of follicle cells (Fig. 3L–L″) and at nurse cell junctions (Fig. 3M–M″). In contrast to wild-type, the rare *Hsp60C^{1}* mutant egg chambers that survived (see below) to later stages also displayed very little Hsp60. The F-actin distribution too was severely affected (Fig. 3M–P, see later). Among the surviving stage 10B and later mutant egg chambers, only approximately 30% (N = 23) showed some accumulation of Hsp60 around the junction of basal nurse cells and oocyte (Fig. 3O) or the future micropyle region (Fig. 3P), which compared with wild-type chambers, was significantly less. Other regions of these late egg chambers showed barely detectable diffuse Hsp60 staining.

Hsp60C^{1} Mutant Egg Chambers Show Variety of Defects in Egg Chambers

Organization of follicle and nurse cells in wild-type, *Hsp60C^{1}*, and *Hsp60C^{1}/Df(2L)Cl-h2* mutant ovarioles was compared (Table 1) by confocal microscopy of DAPI-stained preparations or of egg chambers from females expressing green fluorescent protein (GFP) -tagged Hrb98DE (Morin et al., 2001). We found that the GFP-tagged Hrb98DE protein shows a specific nuclear localization in follicle as well as the nurse cells of all stages of wild-type egg chambers and thus can serve as a good nuclear marker in egg chambers. Until stage 6, the arrangement of follicle cells in *Hsp60C^{1}/Hsp60C^{1}* and *Hsp60C^{1}/Df(2L)Cl-h2* egg chambers (Fig. 4B) appeared generally comparable to that in wild-type (Fig. 4A). However, in all post-stage 6 mutant egg chambers, instead of the regular one-cell-deep layer in wild-type (Fig. 4A; Table 1), the follicle cell layer at the posterior end, although completely covering the oocyte, was irregular and more than one cell deep (Fig. 4B). Interestingly, despite the disorganized follicle cell layer, the identity of polar follicle cells in majority (~98% of 55 stage 6–9 chambers) of mutant egg chambers was not affected as revealed by staining for Fasciclin-III (McGregor et al., 2002; not shown).

Nearly half of stage 7–8 egg chambers from *Hsp60C^{1}/Hsp60C^{1}* or *Hsp60C^{1}/Df(2L)Cl-h2* female flies showed a variety of other defects in addition to the disorganized follicle cell layer (see Table 1) and in agreement with the stage 7–8 of *Drosophila* oogenesis being a developmental checkpoint (Buszczak and Cooley, 2000; Nezis et al., 2000), most of these severely affected egg chambers did not develop further and degenerated (Fig. 4C). The few that survived the stage 7 checkpoint, showed additional defects (see below).

Actin Cytoskeleton Is Affected in *Hsp60C^{1}* Mutant Egg Chambers

The F-actin based cytoskeleton in mutant follicle and nurse cells did not show any detectable difference from that in wild-type until stage 6 (not shown) except for the muscle layer noted above. *Hsp60C^{1}* egg chambers displayed a variety of abnormalities beginning with stage 6–7 when follicle cell remodeling starts. Unlike the regular monolayer of hexagonal follicle cells in wild-type (Fig. 4D), those in the *Hsp60C^{1}/Hsp60C^{1}* egg chambers were highly irregular (Fig. 4E). Most of the mutant egg chambers, including those developing beyond stage 7, showed much less F-actin at nurse cell borders. In some, it was abnormally aggregated around the oocyte (Fig. 4F). Nearly 28% of the 42 surviving post-stage 8 *Hsp60C^{1}/Hsp60C^{1}* egg chambers examined displayed bi- or multinucleate nurse cells (Fig. 4G; Table 1), which may be due to the poor actin reinforcement of cell membranes. Likewise, in some mutant egg chambers, one or more of the nurse cell nuclei appeared to have fallen into the oocyte (not shown).

The F-actin cage, that forms around each of the large nurse cell nucleus (see Fig. 3E) when the nurse cells begin to actively dump their cytoplasmic contents into oocyte, was nearly absent in the mutant stage 10 egg chambers (Fig. 3M). Likewise, the other actin cables, which hold and stabilize ring canals during the rapid cytoplasmic flow in wild-type, were also absent in mutant egg chambers (not shown).

Cell–cell Adhesion Is Affected in *Hsp60C^{1}/Hsp60C^{1}* Egg Chambers

The irregular follicle cell layer and the presence of chambers with mispositioned oocyte (Fig. 4G,H; Table 1) indicate poor cell–cell adhesion in *Hsp60C^{1}/Hsp60C^{1}* or *Hsp60C^{1}/Df(2L)Cl-h2* egg chambers. This was confirmed through immunostaining for some of the cell adhesion markers.

During the cellular rearrangements at stage 7, components of the cadherin adhesion complex, DE-cadherin, Ar-

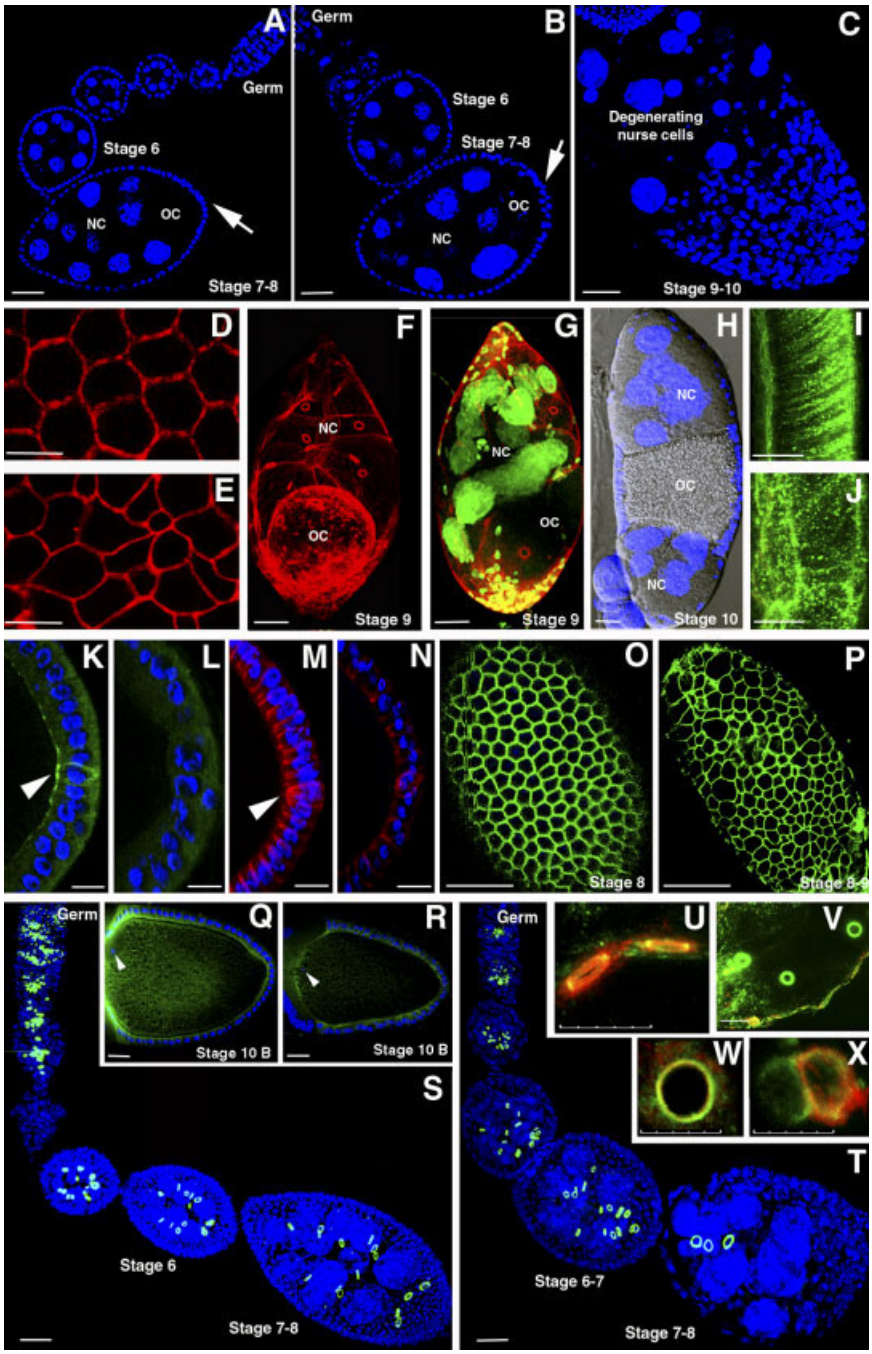

Fig. 4. **A,B:** Confocal images of 4′,6-Diamino-2-phenylindole dihydrochloride (DAPI) stained ovarioles from wild-type (A) and *Hsp60C*^{1} homozygous (B) females. **C:** *Hsp60C*^{1} homozygous stage 9–10 chamber with degenerating nurse cells. **D–F:** Phalloidin-stained follicle cell layer (D,E) and egg chamber (F) from wild-type (D) or *Hsp60C*^{1} mutant (E,F) flies. **G:** Hrb98DE-green fluorescent protein (GFP)-expressing (green) and Phalloidin-stained (red) mid stage egg chamber from *Hsp60C*^{1} mutant female showing bi- and/or multinucleate nurse cells with misplaced oocyte and aberrant F-actin cytoskeleton. **H:** Combined fluorescence and differential interference contrast microscopy image of an egg chamber with a mispositioned oocyte from a mutant fly. **I,J:** Higher magnification lateral views of phosphotyrosine-stained follicle cell layer from wild-type (I) or *Hsp60C*^{1} mutant (J) females. **K–P:** Immunostaining for DE-cadherin (K,L) or Dlg (M,N) or α-spectrin (O,P) in wild-type (K,M,O) and *Hsp60C*^{1} mutant (L,N,P) follicle cell layer (arrowheads mark the posterior pair of polar cells in K,M). **Q,R:** α-Tubulin distribution in wild-type (Q) and *Hsp60C*^{1} mutant (R) oocytes at the 10B stage. **S,T:** Immunostaining for HTS-RC to show status of ring canals in wild-type (S) and *Hsp60C*^{1} mutant (T) ovarioles. **U–X:** Staining of ring canals with anti-phosphotyrosine antibody (green) and Phalloidin (red) from wild-type (U,W) and *Hsp60C*^{1} mutant (V,X) mid-stage nurse cells. Germ, germarium; NC, nurse cells; OC, oocyte. Scale bars = 10 μm in A–C,F–H,O–T,V, 5 μm in D,E,I–N,U,W,X.

madillo, and α-catenin, are known to accumulate along the border between the oocyte and posterior follicle cells to provide the required adhesion between them, and thereby determining the posterior position of the oocyte (Gonzalez-Reyes and St Johnston, 1998; Muller, 2000). Immunostaining of wild-type and mutant egg chambers revealed that unlike the uniform basal expression of DE-cadherin on all follicle cells in wild-type egg chambers and much higher level on the two posterior polar follicle cells, (Fig. 4K), egg chambers from *Hsp60C*^{1}/*Hsp60C*^{1} ovaries had significantly reduced staining, particularly in the posterior polar follicle cells (Fig. 4L). Similarly, compared with wild-type egg chambers (Fig. 4M), the mutant egg chambers showed reduced staining for Dlg, including in the posterior polar follicle cells (Fig. 4N).

Unlike the regular distribution of α-spectrin in wild-type follicle cell layer (Fig. 4O), that in *Hsp60C*^{1}/*Hsp60C*^{1} egg chambers (Fig. 4P) was uneven and disrupted. Likewise, immunostaining for tyrosine phosphorylation, an important regulatory event for formation of cell junctions (Volberg et al., 1992), showed that, while follicle cells in wild-type showed a smooth uniform phosphotyrosine staining of the inner and lateral faces (Fig. 4I), those in *Hsp60C*^{1}/*Hsp60C*^{1} chambers showed uneven and irregular staining with missing columnar arrangement (Fig. 4J).

Hsp60C^{1} Mutation Affects Microtubules and Ring Canals

Posterior follicle cells in wild-type early egg chambers signal the posterior MTOC in oocyte for microtubule remodeling, which is responsible for the localization of several polarity determinants and movement of oocyte nucleus (Riechmann and Ephrussi, 2001; Steinhauer and Kalderon, 2006). Because *Hsp60C*^{1}/*Hsp60C*^{1} egg chambers showed abnormal distribution of actin and cell-adhesion proteins and aberrant arrangement of posterior follicle cells, we examined distribution of microtubules using anti–α-tubulin antibody. In wild-type stage 8–10 oocyte, α-tubulin staining

was seen along the cell membrane. α-tubulin was undetectable in the cytoplasm at the posterior end while a greater concentration was seen at the anterior half, with a stronger presence at the junction of oocyte and nurse cells (Fig. 4Q). On the other hand, more than 80% (N = 25 stage 8–10 egg chambers) of *Hsp60C*^{1}/*Hsp60C*^{1} oocytes showed reduced and somewhat abnormally distributed α-tubulin (Fig. 4R) and in all such cases, the anterodorsal migration of the oocyte nucleus was affected, indicating that the asymmetrical mid-oogenesis microtubule array does not form properly in the mutant chambers.

Status of ring canals in wild-type and *Hsp60C*^{1}/*Hsp60C*^{1} egg chambers was assessed through staining with anti–HTS-RC, TRITC-Phalloidin, anti-Phosphotyrosine, or with anti-Kelch antibodies. Immunostaining with anti–HTS-RC, which exclusively stains the ring canals of developing egg chambers (Robinson et al., 1994), showed obvious differences in the arrangement of ring canals between *Hsp60C*^{1}/*Hsp60C*^{1} (Fig. 4T) and wild-type egg chambers beginning from stage 6 (Fig. 4S), since approximately 80% (N = 24 stage 6–11 chambers) of stage 6 and later *Hsp60C*^{1}/*Hsp60C*^{1} egg chambers showed abnormally located and/or fewer ring canals (Fig. 4T).

In wild-type egg chambers, F-actin accumulates in the inner rim of each ring canal with phosphotyrosine at the outer rim (Fig. 4U,W). In advanced stage *Hsp60C*^{1} mutant egg chambers, some ring canals appeared abnormal with the F-actin staining being more diffuse or nearly absent (Fig. 4V,X). Size of ring canals, however, was not significantly altered in *Hsp60C*^{1}/*Hsp60C*^{1} egg chambers. Anti-Kelch antibody did not show significant differences in staining of ring canals in wild-type and mutant egg chambers (not shown), except for the general defects noted above in the mutant chambers.

Expression and Localization of Hrb98DE, Squid, and Gurken Are Disrupted in *Hsp60C*^{1}/*Hsp60C*^{1} Egg Chambers

The heterogeneous nuclear RNA-binding (hnRNP) and other RNA-binding proteins play significant roles in spatial localization of the various RNAs and proteins in oocyte (Johnstone and Lasko, 2001). Because the *Hsp60C*^{1} mutant egg chambers displayed abnormalities in follicle cell layer and aberrant actin and tubulin distribution in oocyte, we examined expression and localization of two hnRNPs (Hrb98DE and Squid) and Gurken in the mutant egg chambers.

The Hrb98DE and Squid proteins were localized through the *Hrb98DE-GFP* and *Squid-GFP* protein trap alleles, respectively (Morin et al., 2001). The *Hrb98DE-GFP* allele expresses GFP-tagged Hrb98DE in all follicle and nurse cell nuclei starting from stage 1 of oogenesis in wild-type egg chambers (see above). However, Hrb98DE-GFP was nearly absent or significantly reduced in many (~78% of 39 stage 6–11 egg chambers examined) nurse cell nuclei in *Hsp60C*^{1} mutant (*Hsp60C*^{1}/*Hsp60C*^{1}*; Hrb98DE-GFP*/*Hrb98DE-GFP*) egg chambers (compare Fig. 5A with 5B). Interestingly, no significant difference in the nuclear expression of Hrb98DE-GFP was detected in somatic follicle cells of wild-type and the mutant ovarioles (Fig. 5A,B).

Squid binds the gurken mRNA and mediates its transport from nurse cell nucleus to oocyte and as reported earlier (Norvell et al., 2005), the Squid-GFP was nuclear in nurse cells of stage 9–10 egg chambers in wild-type {*w; +/+; Squid-GFP (44-1)*/*Squid-GFP(44-1)*} while it localized at the anterodorsal side and posterior pole in the oocyte (Fig. 5C). In contrast, nearly 80% (N = 32 egg chambers) of the mutant {*w; Hsp60C*^{1}/*Hsp60C*^{1}*; Squid-GFP (44-1)*/*Squid-GFP (44-1)*} stage 9–10 egg chambers showed Squid-GFP in nurse cell cytoplasm as well (Fig. 5D); furthermore, Squid-GFP content was much less in the oocyte and unlike in wild-type (Fig. 5C), its localization there was never specifically restricted to the anterodorsal and posterior sides (Fig. 5D).

The distribution of Gurken in the mutant egg chambers was comparable until stage 6–7 to that in wild-type (not shown). However, compared with the tight localization of Gurken at the anterodorsal corner of the oocyte in wild-type stage 10 egg chambers (Fig. 5E), the majority (~90%, N = 28 stage 7–11 egg chambers) of the post-7 stage mutant egg chambers showed a variety of alterations, like little Gurken in the oocyte but high abundance in nurse cells or scattered distribution of Gurken

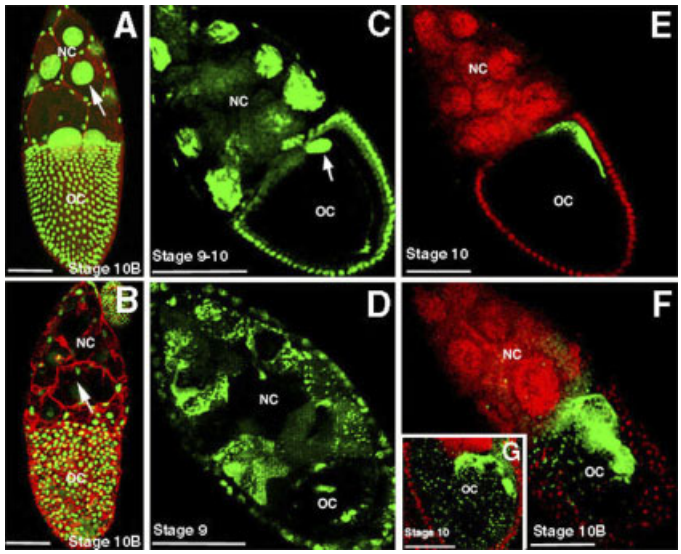

Fig. 5. A–G: Confocal images to show localization of Hrb98DE-GFP (A,B), Squid (C,D), and Gurken (E–G) proteins (green fluorescence in all cases) in wild-type (A,C,E) and *Hsp60C*^{1}/*Hsp60C*^{1} (B,D,F,G) egg chambers. Red fluorescence in A and B shows Phalloidin stained F-actin, while in E–G, red fluorescence shows 4′,6-Diamino-2-phenylindole dihydrochloride (DAPI) -stained nuclei (false colored). Arrow in A indicates a nurse cell nucleus with strong Hrb98DE-green fluorescent protein (GFP) expression, which is highly reduced in case of mutant nurse cells (arrow in B). Arrow in C indicates localization of Squid in the anterodorsal region of wild-type oocyte. NC, nurse cells; OC, oocyte. Scale bars = 50 μm.

throughout the oocyte cytoplasm along with a greater concentration in the anterodorsal region (Fig. 5F,G).

Hsp60C^{1} Mutant Follicle Cell Clones in *Hsp60C*^{1}/+ Egg Chambers Lose Monolayer Arrangement and Show Altered F-Actin Distribution

We generated mitotic clones of follicle cells homozygous for the *Hsp60C*^{1} mutant allele in *Hsp60C*^{1}/+ egg chambers by using FRT/FLP-mediated site-specific somatic recombination (Golic and Lindquist, 1989), to ascertain if the effects of *Hsp60C*^{1} mutation on follicle cell arrangement and F-actin derangement were cell autonomous or result of general weakness of the rare surviving *Hsp60C*^{1} mutant flies. The FLP recombinase was specifically expressed in follicle cells through the *T155-GAL4* transgene (Duffy et al., 1998). The *Hsp60C*^{1}/*Hsp60C*^{1} mitotic clones were identified by the absence of GFP fluorescence in follicle cells. A total of 32 *Hsp60C*^{1}/+ egg chambers derived from several flies and containing variable proportions of *Hsp60C*^{1} homozygous follicle cell clones were examined. In every case, the homozygous *Hsp60C*^{1} follicle cell clones, whether very small or more extensive, exhibited loose and irregular epithelial organization. As seen in the two stage 7 egg chambers in Figure 6A–A″ and B–B″, while the GFP-expressing *Hsp60C*^{1}/+ (or +/+) follicle cells in all clone-bearing egg chambers (N = 32) displayed the regular monolayer arrangement, the GFP-negative *Hsp60C*^{1}/*Hsp60C*^{1} cells, even when only a few (encircled areas in the Fig. 6) had lost the characteristic tight monolayer arrangement. This finding is reminiscent of the disrupted arrangement of follicle cells in *Hsp60C*^{1} homozygous egg chambers (see Fig. 4B,C).

In addition to the altered arrangement of follicle cells, loss of Hsp60C in the *Hsp60C*^{1} mutant clones also affected F-actin membrane cytoskeleton. Figure 6C–C‴ show surface views of an egg chamber bearing multiple *Hsp60C*^{1} mutant follicle cell clones (encircled areas). The F-actin cytoskeleton in each of the *Hsp60C*^{1}/*Hsp60C*^{1} follicle cells was abnormal. Interestingly, the *Hsp60C*^{1}/+ nurse cell nuclei (GFP-positive, Fig. 6D′) in this egg chamber showed extensive apoptotic fragmentation (Fig. 6D), while the F-actin cytoskeleton in them and in the oocyte (Fig. 6D″) was also affected. In all those egg chambers in which *Hsp60C*^{1} mutant clones were small and few, the nurse cells and oocyte appeared unaffected but in those cases where a large proportion of the follicle cells had become *Hsp60C*^{1} homozygous following the FLP-induced somatic recombination, the nurse cells and the oocyte were also affected to varying extent.

Hsp60C^{1} Mutant Germ Cell Clones in *Hsp60C*^{1}/+ Egg Chambers Show Altered F-Actin Distribution and Other Abnormalities

To further examine if *Hsp60C* function is autonomously required in germline cells, mutant germline clones for the *Hsp60C*^{1} allele were generated in *Hsp60C*^{1}/+ egg chambers using the FLP-DFS technique (Chou and Perrimon, 1996). In these clones, the somatic cells are wild-type (*Hsp60C*^{1}/+), whereas the germline cells are homozygous for the *Hsp60C*^{1} mutation. In each such ovary, only one to five ovarioles contained developing egg chambers, confirming that the *ovoD*^{1} mutation was not present in their germline cells, which therefore, were homozygous for the *Hsp60C*^{1} allele.

The germ line clone-bearing egg chambers were stained with DAPI, Hsp60 antibody, and Phalloidin-TRITC to examine the cellular distribution of Hsp60 and F-actin. The *Hsp60C*^{1} homozygous nurse cells and the oocyte in these chambers showed little Hsp60, although the somatic follicle cells had the levels expected in *Hsp60C*^{1}/+ cells (Fig. 7). The overall arrangement of follicle cells was generally comparable to those in wild-type chambers (see inset in Fig. 7A). The frequency of degenerating stage 7 chambers in these mosaic ovaries (~18%, Table 2) was almost 9× greater than that in *Hsp60C*^{1}/+ non-mosaic ovaries (2.2%, Table 1) and comparable to that in *Hsp60C*^{1} homozygotes. The surviving mosaic chambers appeared generally normal until stage 7–8, although the shape and arrangement of F-actin in several of them was affected (Table 2; Fig. 7A). Approximately 35% of stage 9–12 chambers were also seen to be degenerating (inset in Fig. 7C). Phalloidin staining showed that the F-actin network in nurse cells and oocyte in most of the surviving mid-stage mosaic egg chambers was weak and irregular (Fig. 7A–C, compare with Fig. 3F–P). The accumulation of Hsp60 protein around the junction of basal nurse cells and anterior oocyte margin during later stages of oogenesis seen in wild-type (Fig. 3F,G) was absent in the surviving *Hsp60C*^{1} germ line mosaic egg chambers (Fig. 7C,D) and further unlike wild-type, the F-actin at this junction was more on the oocyte side rather than the nurse cell side (compare Figs. 3G and 7C). Interestingly, like in *Hsp60C*^{1}/*Hsp60C*^{1} chambers (Fig. 3M), the germ cell clone bearing egg chambers (Fig. 7C,D) also failed to develop the F-actin cables to hold the large nurse cell nuclei at later stages of oogenesis, which is characteristically seen in wild-type (Fig. 3E) or *Hsp60C*^{1}/+ egg chambers. Approximately 14% of the stage 8–9 egg chambers showed misplaced oocyte (Table 2). In some of the mosaic chambers with more severely disorganized F-actin cytoskeleton in nurse cells, the follicle cells also showed abnormalities and signs of degeneration (see inset in Fig. 7C).

DISCUSSION

The present study clearly demonstrates that the *Hsp60C* gene expresses in a dynamic pattern through oogenesis and that homozygosity for the *Hsp60C*^{1} recessive loss of function allele (Sarkar and Lakhotia, 2005) results in severe defects in oogenesis and, thus, in complete sterility of the homozygous mutant females. Restoration of fertility and other phenotypes associated with the *Hsp60C*^{1} allele upon excision of the P-transposon (Sarkar and Lakhotia, 2005) and a similar or a little more exaggerated oogenesis phenotype (Table 1) when this mutant allele is placed against the *Df(2L)cl-h2* deficiency, which covers this gene's location (Lindsley and Zimm, 1992), confirm that the abnor-

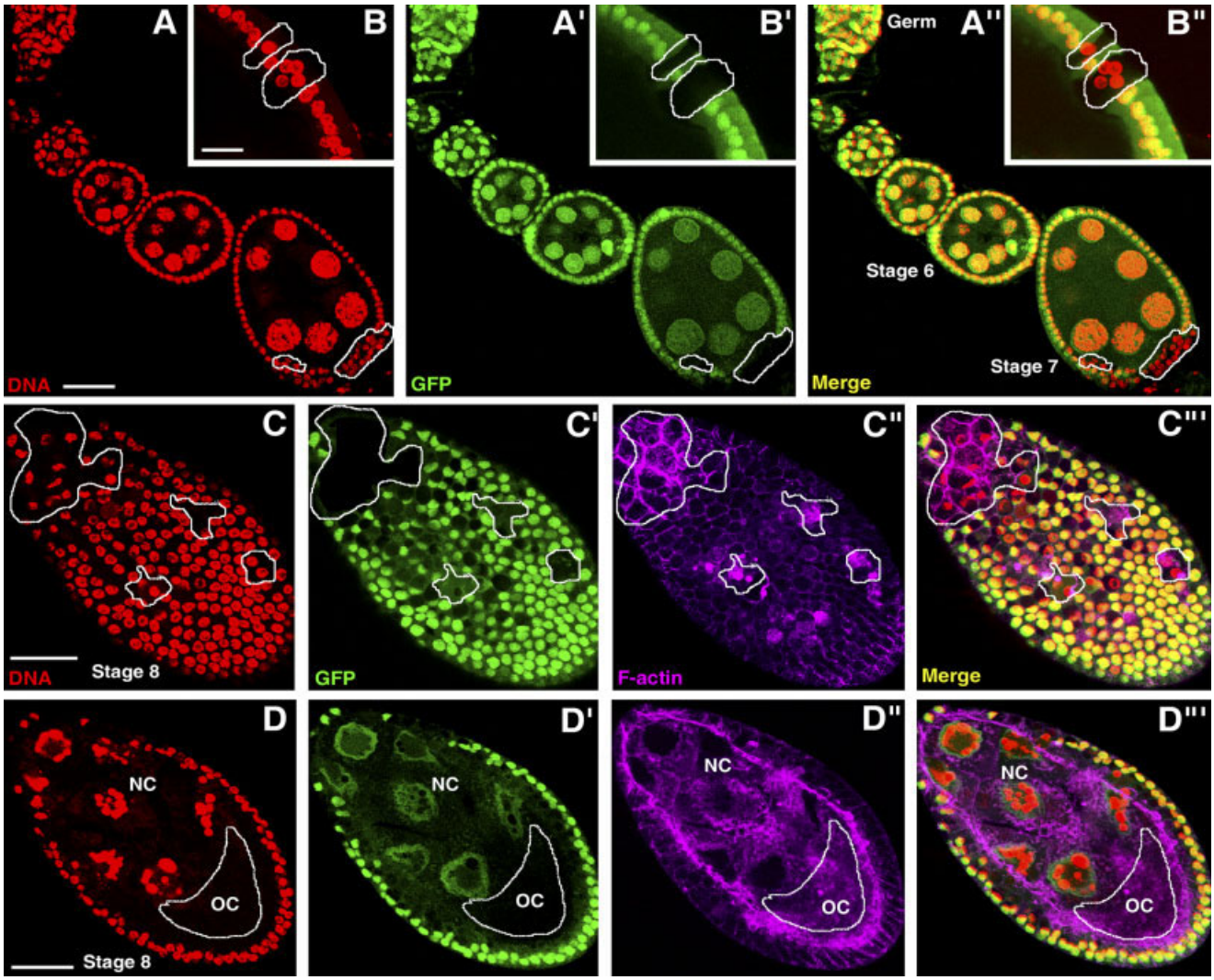

Fig. 6.

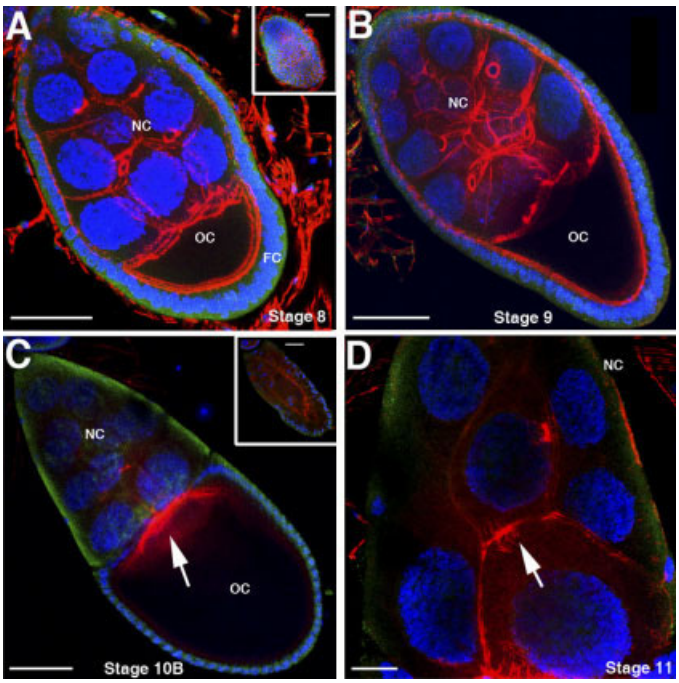

Fig. 7.

malities in oogenesis in the surviving $Hsp60C^1/Hsp60C^1$ homozygous females are indeed due to the *Hsp60C* mutant allele. Because the mature egg does not show any detectable Hsp60C transcripts or the protein, the Hsp60C appears to have functions in oogenesis rather than having maternally transmitted zygotic functions.

As noted earlier (Sarkar and Lakhotia, 2005), only approximately 10% of the $Hsp60C^1$ homozygotes survive as weak and short-lived flies. Because the general physiology of flies is known to significantly affect progression of oogenesis, it remains possible that the observed defects in oogenesis in the $Hsp60C^1$ homozygous females result merely from their poor physiology. Present results, however, rule out the possibility that defective oogenesis

Developmental Dynamics

TABLE 2. Defects in *Hsp60C*^{1} Homozygous Mutant Germline Clones in *Hsp60C*$^{+}$/Hsp60C^{1} Egg Chambers

Stage	Total egg chambers	Degenerating chambers	Surviving chambers	
			Nurse cells and oocyte	Follicle cells
Until stage 8	38	7	No major defect, except some alterations in egg chamber shape and/or some defects in F-actin arrangement	normal in most cases
Stage 9-10	22	10	Severe defects in arrangement of F actin in nurse cells	
			Abnormal positioning of oocyte in 3 egg chambers	Organization affected in severely affected and degenerating egg chambers
Stage 11-12	8	2	Defective F-actin cage No accumulation of Hsp60 protein at anterior border of oocyte	
			Positioning of oocyte nucleus not affected	Organization affected in severely affected and degenerating egg chambers
Stage 12-14	6	.	All abnormal showing dump less and polarity defect phenotypes	

in *Hsp60C*^{1} homozygous females is a nonspecific effect of general weakness/poor physiology of the mutant flies. Comparison of immunostaining of wild-type and *Hsp60C*^{1} homozygous egg chambers with the SPA805 anti-Hsp60 antibody, which is expected to detect all the four Hsp60 family members in *D. melanogaster* cells (Lakhotia et al., 2002), suggests that Hsp60C contributes maximally to the Hsp60 family proteins detected by this antibody in egg chambers and striated muscles. The remarkable cell type and stage-specific expression of *Hsp60C* gene in follicle as well as germline cells in egg chambers but not in other parts of the female reproductive system correlates with the fact that only the egg chambers, but not the accessory gland, oviduct, etc., are severely affected by the *Hsp60C*^{1} mutation. Finally, clonal analyses made it clear that Hsp60C function is essential in the follicle as well as in the germline cells because in both kinds of mosaics, autonomous defects in F-actin cytoskeleton and other aspects of oogenesis were seen and in both cases, the mosaic egg chambers failed to complete oogenesis. Therefore, it is obvious that the aberrations seen in *Hsp60C*^{1} homozygous egg chambers are largely due to this protein's essential functions during oogenesis rather than to the poor physiology of the escapee survivors.

Abnormalities in the *Hsp60C*^{1} mutant egg chambers first become apparent after stage 5–6 in the form of misorganized posterior follicle cells, and this finding correlates well with a significant reduction in Hsp60C transcripts in the mutant follicle cells from stage 5–6 onward. Although the mutant germ cells did not show Hsp60C transcripts even during stage 1–4, any ensuing abnormality in their functions may not result in easily detectable phenotype at this early stage. The follicle cells have significant roles in organization of egg chamber from the very early stage, and they are especially important in converting the rounded stage 5–6 chambers to anteroposteriorly elongated later stage chambers. Therefore, any misfunctioning of the follicle cells at this early stage will have cascading effects on subsequent development of egg chamber.

The most significant abnormalities observed in *Hsp60C*^{1} mutant or mo-

Fig. 6. A–D: Follicle cells in *Hsp60C*^{1}/*Hsp60C*^{1} clones, generated by FLP-mediated somatic recombination, in *Hsp60C*^{1}/+ egg chambers are irregularly arranged and show abnormal F-actin cytoskeleton. A–A″ and B–B″ (only a part of the follicle cell layer is shown in B) are examples of small *Hsp60C*^{1}/*Hsp60C*^{1} clones in two different stage 7 egg chambers (green fluorescent protein [GFP] -negative encircled areas) and in each of the clones, the monolayer arrangement of the mutant follicle cells is disrupted; A,B show 4′,6-Diamino-2-phenylindole dihydrochloride (DAPI) fluorescence (red, pseudo-color), A′,B′ show GFP fluorescence, while A″ and B″ are DAPI and GFP merged images. C–C‴ show surface views of DAPI (C, red pseudo-color), GFP (C′, green), tetrarhodamine isothiocyanate (TRITC) -Phalloidin (C″, magenta pseudo-color) fluorescence of a stage 8 *Hsp60C*^{1}/+ egg chamber with multiple *Hsp60C*^{1}/*Hsp60C*^{1} mitotic clones in the follicle cell layer (encircled areas); C‴ shows a merged image of C–C″. Note the disruption in regular monolayer arrangement and aberrant accumulation of F-actin in all the *Hsp60C*^{1} homozygous follicle cell clones. D–D‴ show mid-plane optical section of the same egg chamber as in C–C‴ displaying fragmentation (apoptosis) of nurse cell nuclei even though they are GFP-positive and, therefore, *Hsp60C*^{1}/+; the oocyte area is encircled. Germ, germarium; NC, nurse cells; OC, oocyte. Scale bars = 10 μm in A–A″,C–D″, 5 μm in B–B″.

Fig. 7. Confocal images of FLP-DFS technique-generated germline mosaic egg chambers of the indicated stages stained with 4′,6-Diamino-2-phenylindole dihydrochloride (DAPI, blue), Phalloidin-tetrarhodamine isothiocyanate (TRITC; red) and immunostained with anti-Hsp60 antibody (green). Note the normal distribution of Hsp60 in follicle cells (FC, *Hsp60C*^{1}/+), but its near absence in nurse cells (NC) and developing oocytes (OC), all of which are Hsp60C1 homozygous. The actin filaments in *Hsp60C*^{1} homozygous nurse cells and the oocyte (germline clones) are abnormally arranged. The inset in A shows the surface image of the chamber shown in A to illustrate the near normal arrangement of follicle cell layer, although the nurse cells and the oocyte show somewhat abnormal actin distribution and the chamber shape is affected. The inset in C shows a degenerating mid-stage egg chamber. The arrow in C points to the rather diffuse accumulation of F-actin at junction of nurse cells and oocyte, while that in D points to the poorly developed actin cage in nurse cell of a stage 11 chamber. Scale bars in A,C,D = 50 μm, 10 μm in D.

saic egg chambers are (1) poor adhesion of follicle cells from stage 6–7 onward, (2) membrane fragility of nurse cells, (3) aberrations in ring canals, (4) poorly developed F-actin cables that cage the large polyploid nurse cell nuclei during the dumping process, and (5) impaired polarity in developing oocyte. It is interesting that all these abnormalities can result, in a cascading manner or independently, from defective organization of the various cytoskeletal elements during the progression of oogenesis. In this context, the overlapping distribution of Hsp60, F-actin, and/or α-tubulin, in follicle and germline cells in egg chambers, especially near cell membranes and at sites where MTOCs develop, is significant. Although these different proteins did not show absolute colocalization, that they were largely present in overlapping domains and these domains developed defects in the absence of Hsp60C indicate that Hsp60C is required for normal organization of cytoskeletal components during progression of normal oogenesis. It is notable in this context that an essential requirement of Hsp60 family proteins for proper folding and stability of actin and tubulin proteins and for organization of cytoskeletal elements in yeast and other eukaryotes has already been shown (Chen et al., 1994; Melki and Cowan, 1994; Vinh and Drubin, 1994; Liang and MacRae, 1997; Sarkar et al., 2006). Furthermore, Hsp60 family proteins, immunoprecipitated with the same anti-Hsp60 antibody as used by us, were found to bind most strongly with actin in *C. elegans* (Leroux and Candido, 1997). Considering all these, we believe that the Hsp60C is necessary for proper organization of the F-actin and other cytoskeletal elements in different cell types of egg chambers. Various abnormalities seen in egg chambers of *Hsp60C*^{1} mutant chambers thus seem to be direct or indirect consequences of cytoskeletal abnormalities. The mode of interaction between Hsp60C and cytoskeletal components remains to be analyzed.

The cytoskeletal elements and cadherin-mediated differential adhesion of the follicle cells are critical for their proliferation, migration, remodeling, fate adaptation, and for communication with nurse cells and the growing oocyte (Zhang and Kalderon, 2000; Steinhauer and Kalderon, 2006). Several actin-binding proteins are known to be essential for maintenance of cellular integrity and follicle cell morphogenesis during *Drosophila* oogenesis (Hudson and Cooley, 2002). It is, therefore, likely that absence of Hsp60C and consequent inappropriate organization of F-actin components effect follicle cell adhesion, with the first effect being manifest at the posterior pole around stage 6–7, when the level of Hsp60C transcripts also significantly declines in follicle cells (see Fig. 2). During remodeling of egg chambers at these stages, follicle cells at the posterior pole face greater strain due to curvature and, therefore, the posterior polar cells require longer septate junctions than their lateral counterparts (Mahowald, 1972). The weak septate junctions seen in the posterior pole cells in the mutant stage 6–7 chambers obviously do not provide the required strong cell–cell adhesion and thus result in irregular epithelium. Mutations in genes encoding cell adhesion molecules such as Armadillo, DE-cadherin, Merlin, α-Spectrin, etc. affect follicle cell remodeling (Oda et al., 1997; Muller, 2000; MacDougall et al., 2001; Hudson and Cooley, 2002; Steinhauer and Kalderon, 2006), and the resulting phenotypes are in several ways similar to those seen in the *Hsp60C*^{1} mutant egg chambers. In addition to the posterior group of follicle cells, Hsp60C is also essential for generating and maintaining a patterned monolayer of all other follicle cells as evidenced by the irregular arrangement of *Hsp60C*^{1}/*Hsp60C*^{1} follicle cells in mitotic clones, irrespective of their location and size (Fig. 6). Mispositioning of oocyte in some *Hsp60C*^{1} egg chambers also reflects defective adhesion of follicle cells with the oocyte. The nonautonomous perturbations in *Hsp60C*^{1}/+ nurse cells in follicle cell mosaics and in follicle cells in germline mosaics at later stages of oogenesis too reflect the need for appropriate interactions between follicle cell monolayer and the enclosed germline cells (Muller, 2000).

The weak or defective F-actin network associated with the various cell membranes in *Hsp60C*^{1} egg chambers also appear responsible for ring canal aberrations, the fragility of nurse cell membranes and for the dumpless phenotype shown by the few surviving late stage chambers. Defects in distribution and/or numbers of ring canals even at stage 6 in *Hsp60C*^{1} mutant egg chambers (Fig. 4T) reflect defective membrane dynamics during nurse cell division and early development, presumably due to the near complete absence of Hsp60C transcripts in germline cells from stage 1 (Fig. 2). The frequent occurrence of bi- or multinucleate nurse cells or of the nurse cell nucleus falling into the oocyte in the mutant chambers also indicate fragility of nurse cell membranes, presumably because of insufficient or misorganized F-actin. It appears that, in the absence of appropriately continuing F-actin folding/maturation, the ring canals, even after their initial assembly, may lose stability and degenerate in the surviving later stages.

Signaling by the polarized posterior epithelial follicle cells is required for establishing the posterior MTOC in oocyte and its later remodeling (Chekulaeva and Ephrussi, 2004). The MTOC in turn is important for establishing both the anteroposterior and dorsoventral egg axes in *Drosophila* (van Eeden and St Johnston, 1999; Riechmann and Ephrussi, 2001; Chekulaeva and Ephrussi, 2004). The altered distribution of α-tubulin in oocyte in the mutant egg chambers reflects defective remodeling of posterior MTOC, presumably because of aberrant signaling by the overlying disorganized follicle cell layer and defective tubulin maturation in absence of Hsp60C. The remarkable similarity between the reported localization site of γ-tubulin (Schnorrer et al., 2002) and Hsp60 and F-actin near the basal nurse cell cytoplasm and anterior oocyte cortex at the beginning of stage 10B, seen in the present study, is significant. Although we did not study the distribution of γ-tubulin in the mutant chambers, that of F-actin at the junction of nurse cells and oocyte was found to be affected in the mutant stage 10B-12 chambers. This finding indicates that Hsp60C plays an important role in the formation of the MTOC at this region also in wild-type egg chambers. The near absence of

Hsp60C in the *Hsp60C*^{1} mutant egg chambers may thus affect the various MTOCs that develop in the oocyte at different developmental stages. The defective MTOCs would affect several microtubule-dependent developmental processes like localization of proteins like Squid and Gurken, and of the oocyte nucleus during mid and late oogenesis. That the disorganized posterior follicle cells in stage 6–7 *Hsp60C*^{1} mutant egg chambers affect the posterior MTOC remodeling is also evidenced by the fact that, in germline mosaic egg chambers that have a normal follicle cell layer, the oocyte nuclear position remains normal (Table 2). Consequent to mislocalization of Squid, Gurken, and the oocyte nucleus in mutant chambers, egg polarity will be affected, as reflected in abnormal dorsal appendages in the few eggs that can be recovered. It will be interesting to further examine if Hsp60C has a direct role also in the transport and characteristic localization of proteins like Squid, Gurken, and so on, in oocyte.

We are not aware of any previous report describing a patterned localization of Hsp60 on A-bands of skeletal muscles. However, the patterned localization of Hsp60 in normal skeletal muscles and the disorganized state of these muscles in absence of Hsp60C protein are suggestive of an important role of this member of the Hsp60 family protein in proper organization of actin and myosin filaments in skeletal muscles of flies. Since normal muscular organization and its neural co-ordination have been reported to be essential for egg development and oviposition (Middleton et al., 2006), it remains possible that the misorganized striated muscle fibers that wrap germarium and the egg chambers in *Hsp60C*^{1} mutant flies may also affect oogenesis. The poor musculature in the oviduct of the mutant flies may hinder egg laying.

Our studies show, for the first time, that the Hsp60C protein is essential at multiple steps of oogenesis, which seem to relate primarily to cytoskeletal structures in follicle as well as nurse cells. In our earlier study (Sarkar and Lakhotia, 2005) on the effects of the *Hsp60C*^{1} mutation on tracheal morphogenesis and spermatogenesis, we raised the possibility that the Hsp60C itself may also function as a signaling molecule, especially because such a function is known in other systems (Gobert et al., 2004; Sarkar et al., 2006). In addition to the possible signaling activity, the Hsp60C also appears to have essential roles in organization of the various F-actin, tubulin, and other cytoskeletal elements during oogenesis. Further studies will help understand how the Hsp60C performs its diverse vital functions in development and differentiation in *Drosophila*.

EXPERIMENTAL PROCEDURES

Drosophila Stocks

The different stocks used in this study, either available in laboratory or obtained from the Bloomington stock center or other sources, were maintained on standard *Drosophila* food medium at 22 ± 1°C. *Oregon R*$^{+}$ served as wild-type control. *Hsp60C*^{1} is a recessive lethal loss of function allele of the *Hsp60C* gene, in which a P-transposon is inserted at −251-bp position in the promoter region (Sarkar and Lakhotia, 2005). The *Df(2L)cl-h2* chromosome carries a deletion of the 25D06 to 25F04-05 region (Lindsley and Zimm, 1992), which covers the *Hsp60C* locus (Sarkar and Lakhotia, 2005), *w; + / +; Hrb98DE-GFP (ZCL 0588)/Hrb98DE-GFP (ZCL 0588)* and *w; + / +; Squid-GFP (44-1)/ Squid-GFP (44-1)* are protein-trap lines in which the Hrb98DE and Squid hnRNP family proteins, respectively, are tagged with GFP (Morin et al., 2001). Appropriate crosses were made to generate *w; Hsp60C*^{1}*/CyO; Hrb98DE-GFP (ZCL 0588)/Hrb98DE-GFP (ZCL 0588)* and *w; Hsp60C*^{1}*/ CyO; Squid-GFP (44-1)/Squid-GFP (44-1)* stocks.

For generation of mitotic clones of *Hsp60C*^{1} homozygous follicle cells, *w*^{1118}*; P{ry*$^{+t7.2}$*=neoFRT}40A/CyO* (Xu and Rubin, 1993), and *w*^{1118}*; P{Ubi-GFP}33 P{Ubi-GFP}38 P{neoFRT}40A/ CyO; P{GawB}T155 P{UAS-FLP1.D} JD2/TM3, Sb*^{1} stocks (Duffy et al., 1998) were used. For generation of *Hsp60C*^{1} mutant germline clones, *w*^{1118}*; P{ry*$^{+t7.2}$*=neoFRT}40A/CyO and w* P{ry[+t7.2]=hsFLP}12; P{w[+mC] =ovoD1-18}2La P{w[+mC]=ovoD1-18} 2Lb P{ry[+t7.2]=neoFRT}40A /CyO* stocks (Chou and Perrimon, 1996) were used.

Generation of *Hsp60C*^{1}*/Hsp60C*^{1} Homozygous Follicle or Germline Cell Clones in *Hsp60C*^{1}/+ Egg Chambers

Homozygous *Hsp60C*^{1} mutant follicle cell clones were generated by the Gal4-directed and UAS-FLP–mediated site-specific mitotic recombination technique (Golic and Lindquist, 1989). Follicle cell clones mutant for *Hsp60C*^{1} were generated using the *T155Gal4/UAS-FLP* transgene inserted on chromosome 3, which drives expression of the site-specific yeast recombinase FLP in all the follicle cells during oogenesis (Duffy et al., 1998). The *Hsp60C*^{1} mutant allele was recombined onto the *P{ry*$^{+t7.2}$*=neoFRT}40A* carrying chromosome through appropriate crosses. The *w*^{1118}*; P{ry*$^{+t7.2}$*=neoFRT}40A Hsp60C*^{1}*/CyO; + / +* flies were crossed with *w*^{1118}*; P{Ubi-GFP}33 P{Ubi-GFP}38 P{neoFRT}40A Hsp60C*$^{+}$*/CyO; P{GawB}T155 P{UAS-FLP1.D}JD2/ TM3, Sb*^{1} flies. In the progeny, *w*^{1118}*/ w*^{1118}*; Hsp60C1 P{ry*$^{+t7.2}$*=neoFRT}40A /Hsp60C*$^{+}$ *P{Ubi-GFP}33 P{Ubi-GFP} 38 P{neoFRT}40A; P{GawB}T155 P{UAS-FLP1.D}JD2/ +* female flies (non-curly wings and non-stubble) were identified and their egg chambers examined for presence of clones of *Hsp60C*^{1} homozygous follicle cells. The mutant mitotic clones were recognized by the absence of nuclear GFP fluorescence, which was shown by all *Hsp60C*^{1}/+ cells or the +/+ mitotic clones. The egg chambers were stained with TRITC-Phalloidin and/or DAPI for examination by confocal microscopy (see below).

Homozygous *Hsp60C*^{1} germline clones were generated using the FLP-DFS technique (Chou and Perrimon, 1996). The *w*^{1118}*; Hsp60C*^{1} *P{ry*$^{+t7.2}$*= neoFRT}40A/CyO* female flies were crossed to *y*^{1} *w* P{ry[+t7.2]=hsFLP} 12; Hsp60C*$^{+}$ *P{w[+mC]=ovoD1-18} 2LaP{w[+mC]=ovoD1-18}2Lb P{ry [+t7.2]=neoFRT}40A /CyO* males. Clones were induced by exposing third instar larvae at 37°C for 2 hr on 2 consecutive days. Ovaries from 3–5

days adult non-curly progeny females (y^1 *w* P{ry[+t7.2]=hsFLP}12/*w^{1118}*; $Hsp60C^+$ P{w[+mC]=ovoD1-18}2La P{w[+mC]=ovoD1-18}2Lb P{ry [+ t7.2] =neoFRT}40A/$Hsp60C^1$P {$ry^{+t7.2}$= neoFRT}40A) were dissected and examined by confocal microscopy after staining with DAPI, Phalloidin-TRITC, and anti–Hsp60-antibody (see below). Egg chambers from sister non-curly flies that did not receive heat shock during third instar stage were examined as control.

RNA:RNA In Situ Hybridization With Adult Female Reproductive Organs

An *Hsp60C* specific digoxigenin (DIG) -labeled riboprobe (Sarkar and Lakhotia, 2005) was used for hybridization in situ with cellular RNA in wild-type and $Hsp60C^1$ homozygous mutant adult female reproductive organs. Ovaries and the associated organs were hand-dissected from 2-day-old females (wild-type and $Hsp60C^1$/$Hsp60C^1$) and fixed in 1:3 mixture of 4% formaldehyde:heptane for 20 min. Subsequent steps for RNA:RNA in situ hybridization were carried out as described earlier (Sarkar and Lakhotia, 2005). The hybridization was detected either chromogenically, using alkaline-phosphatase–conjugated anti-DIG antibody (Roche Applied Science, Germany) or by multiphoton confocal microscopy (Bio-Rad Radiance 2100) after binding with fluorescein isothiocyanate (FITC) -conjugated anti-DIG antibody (Roche Applied Science, Germany).

GFP Localization and Immunostaining of Egg Chambers

Ovaries dissected from 2-day-old female flies of the desired genotypes (and expressing GFP) were fixed in 4% paraformaldehyde in PBS (18.6 mM NaH_2PO_4, 84.1mM Na_2HPO_4, 17.5 mM NaCl). After 3 × 10 min washing in PBTX (PBS, 0.1% Triton X-100 and 0.1% bovine serum albumin), they were mounted in antifade solution for confocal microscopy.

The antibodies used for immunostaining were: anti–Fas-III (1:10; Patel et al., 1987), anti-Gurken (1:30; Queenan et al., 1999), anti-Dlg (1:20; Goode and Perrimon, 1997), anti–Hts-RC (1:1; Robinson et al., 1994), anti–α-spectrin (1:50; Dubreuil et al., 1987), anti–DE-Cadherin (1:20; Oda et al., 1997), all obtained from Developmental Studies Hybridoma Bank (USA); the other antibodies were Mouse monoclonal Anti-Phosphotyrosine (1:100, Santa Cruz, CA), monoclonal anti–α-tubulin-FITC Conjugate (DM1A, 1:250, SIGMA), and rabbit polyclonal anti-Hsp60 (SPA 805, 1:100, Stressgen, Canada).

For immunostaining, ovaries from 2-day-old adult wild-type and $Hsp60C^1$/$Hsp60C^1$ females were fixed and processed for immunofluorescent staining as described earlier (Sarkar and Lakhotia, 2005). After binding with the desired primary antibody, the ovaries were incubated for 1 hr at room temperature in the appropriate Alexa fluor–conjugated secondary antibody (1:200 dilution, Molecular Probes, New Brunswick, NJ), after which the ovaries were counterstained with DAPI (1 μg/ml, Molecular Probes) to visualize nucleus. For F-actin staining, fixed/immunostained ovaries were incubated with TRITC-conjugated Phalloidin (8 U/ml in PBS, Sigma, St. Louis, MO) for 30 min at room temperature in the dark. All fluorescently stained tissues were mounted in antifade (Molecular Probes) and observed with a Bio-Rad Radiance 2100 multiphoton confocal microscope.

ACKNOWLEDGMENTS

We thank Bloomington *Drosophila* Stock Center and Dr. Xavier Morin (Cambridge) for fly stocks. We also thank the anonymous reviewers and the corresponding editor, Dr. Ken Irvine, for critical comments and suggestions. This work is supported by research grant from Department of Biotechnology, Government of India, New Delhi, to S.C.L. and by the Department of Science and Technology, Government of India, New Delhi, through its support for the Multiphoton Confocal Microscope National Facility. S.S. was supported by a research fellowship from the Council of Scientific and Industrial Research, New Delhi.

REFERENCES

Arya R, Mallik M, Lakhotia SC. 2007. Heat shock genes - integrating cell survival and death. J Biosci 32:595–610.

Betran E, Thornton K, Long M. 2002. Retroposed new genes out of the X in Drosophila. Genome Res 12:1854–1859.

Buszczak M, Cooley L. 2000. Eggs to die for: cell death during Drosophila oogenesis. Cell Death Differ 7:1071–1074.

Chekulaeva M, Ephrussi A. 2004. Drosophila development: RNA interference ab ovo. Curr Biol 14:R428–R430.

Chen X, Sullivan DS, Huffaker TC. 1994. Two yeast genes with similarity to TCP-1 are required for microtubule and actin function in vivo. Proc Natl Acad Sci U S A 91:9111–9115.

Chou TB, Perrimon N. 1996. The autosomal FLP-DFS technique for generating germline mosaics in Drosophila melanogaster. Genetics 144:1673–1679.

Dubreuil R, Byers TJ, Branton D, Goldstein LS, Kiehart DP. 1987. Drosophilia spectrin. I. Characterization of the purified protein. J Cell Biol 105:2095–2102.

Duffy JB, Harrison DA, Perrimon N. 1998. Identifying loci required for follicular patterning using directed mosaics. Development 125:2263–2271.

Gobert AP, Bambou JC, Werts C, Balloy V, Chignard M, Moran AP, Ferrero RL. 2004. Helicobacter pylori heat shock protein 60 mediates interleukin-6 production by macrophages via a toll-like receptor (TLR)-2-, TLR-4-, and myeloid differentiation factor 88-independent mechanism. J Biol Chem 279:245–250.

Golic KG, Lindquist S. 1989. The FLP recombinase of yeast catalyzes site-specific recombination in the Drosophila genome. Cell 59:499–509.

Gonzalez-Reyes A, St Johnston D. 1998. The Drosophila AP axis is polarised by the cadherin-mediated positioning of the oocyte. Development 125:3635–3644.

Goode S, Perrimon N. 1997. Inhibition of patterned cell shape change and cell invasion by Discs large during Drosophila oogenesis. Genes Dev 11:2532–2544.

Hartl FU, Hayer-Hartl M. 2002. Molecular chaperones in the cytosol: from nascent chain to folded protein. Science 295:1852–1858.

Hudson AM, Cooley L. 2002. Understanding the function of actin-binding proteins through genetic analysis of Drosophila oogenesis. Annu Rev Genet 36:455–488.

Johnstone O, Lasko P. 2001. Translational regulation and RNA localization in Drosophila oocytes and embryos. Annu Rev Genet 35:365–406.

King RC. 1970. The meiotic behavior of the Drosophila oocyte. Int Rev Cytol 28:125–168.

Lakhotia SC, Srivastava P, Prasanth KV. 2002. Regulation of heat shock proteins, Hsp70 and Hsp64, in heat-shocked Malpighian tubules of Drosophila melanogaster larvae. Cell Stress Chaperones 7:347–356.

Leroux MR, Candido EP. 1997. Subunit characterization of the Caenorhabditis

elegans chaperonin containing TCP-1 and expression pattern of the gene encoding CCT-1. Biochem Biophys Res Commun 241:687–692.

Liang P, MacRae TH. 1997. Molecular chaperones and the cytoskeleton. J Cell Sci 110(Pt 13):1431–1440.

Lindsley DL, Zimm GG. 1992. In: The genome of *Drosophila melanogaster*. San Diego: Academic Press.

MacDougall N, Lad Y, Wilkie GS, Francis-Lang H, Sullivan W, Davis I. 2001. Merlin, the Drosophila homologue of neurofibromatosis-2, is specifically required in posterior follicle cells for axis formation in the oocyte. Development 128:665–673.

Maguire M, Coates AR, Henderson B. 2002. Chaperonin 60 unfolds its secrets of cellular communication. Cell Stress Chaperones 7:317–329.

Mahowald AP. 1972. Ultrastructural observations on oogenesis in Drosophila. J Morphol 137:29–48.

McGregor JR, Xi R, Harrison DA. 2002. JAK signaling is somatically required for follicle cell differentiation in Drosophila. Development 129:705–717.

Melki R, Cowan NJ. 1994. Facilitated folding of actins and tubulins occurs via a nucleotide-dependent interaction between cytoplasmic chaperonin and distinctive folding intermediates. Mol Cell Biol 14:2895–2904.

Middleton CA, Nongthomba U, Parry K, Sweeney ST, Sparrow JC, Elliott CJ. 2006. Neuromuscular organization and aminergic modulation of contractions in the Drosophila ovary. BMC Biol 4:17.

Morin X, Daneman R, Zavortink M, Chia W. 2001. A protein trap strategy to detect GFP-tagged proteins expressed from their endogenous loci in Drosophila. Proc Natl Acad Sci U S A 98:15050–15055.

Muller HA. 2000. Genetic control of epithelial cell polarity: lessons from Drosophila. Dev Dyn 218:52–67.

Nezis IP, Stravopodis DJ, Papassideri I, Robert-Nicoud M, Margaritis LH. 2000. Stage-specific apoptotic patterns during Drosophila oogenesis. Eur J Cell Biol 79: 610–620.

Norvell A, Debec A, Finch D, Gibson L, Thoma B. 2005. Squid is required for efficient posterior localization of oskar mRNA during Drosophila oogenesis. Dev Genes Evol 215:340–349.

Oda H, Uemura T, Takeichi M. 1997. Phenotypic analysis of null mutants for DE-cadherin and Armadillo in Drosophila ovaries reveals distinct aspects of their functions in cell adhesion and cytoskeletal organization. Genes Cells 2:29–40.

Patel NH, Snow PM, Goodman CS. 1987. Characterization and cloning of fasciclin III: a glycoprotein expressed on a subset of neurons and axon pathways in Drosophila. Cell 48:975–988.

Peifer M, Orsulic S, Sweeton D, Wieschaus E. 1993. A role for the Drosophila segment polarity gene armadillo in cell adhesion and cytoskeletal integrity during oogenesis. Development 118:1191–1207.

Perezgasga L, Segovia L, Zurita M. 1999. Molecular characterization of the 5′ control region and of two lethal alleles affecting the hsp60 gene in Drosophila melanogaster. FEBS Lett 456:269–273.

Queenan AM, Barcelo G, Van Buskirk C, Schupbach T. 1999. The transmembrane region of Gurken is not required for biological activity, but is necessary for transport to the oocyte membrane in Drosophila. Mech Dev 89:35–42.

Ranson NA, White HE, Saibil HR. 1998. Chaperonins. Biochem J 333:233–242.

Riechmann V, Ephrussi A. 2001. Axis formation during Drosophila oogenesis. Curr Opin Genet Dev 11:374–383.

Robinson DN, Cant K, Cooley L. 1994. Morphogenesis of Drosophila ovarian ring canals. Development 120:2015–2025.

Sarkar S, Lakhotia SC. 2005. The Hsp60C gene in the 25F cytogenetic region in Drosophila melanogaster is essential for tracheal development and fertility. J Genet 84:265–281.

Sarkar S, Arya R, Lakhotia SC. 2006. Chaperonins: in life and death. In: Sreedhar AS, Srinivas UK, editors. Stress responses: a molecular biology approach. Trivandrum, India: Signpost. p 43–60.

Schnorrer F, Luschnig S, Koch I, Nusslein-Volhard C. 2002. Gamma-tubulin37C and gamma-tubulin ring complex protein 75 are essential for bicoid RNA localization during drosophila oogenesis. Dev Cell 3:685–696.

Spradling A. 1993. Developmental genetics of oogenesis. In: Bate M, Martinez-Arias A, editors. The development of *Drosophila melanogaster*. New York: Cold Spring Harbor Press. p 1–70.

Steinhauer J, Kalderon D. 2006. Microtubule polarity and axis formation in the Drosophila oocyte. Dev Dyn 235:1455–1468.

Timakov B, Zhang P. 2001. The hsp60B gene of Drosophila melanogaster is essential for the spermatid individualization process. Cell Stress Chaperones 6: 71–77.

van Eeden F, St Johnston D. 1999. The polarisation of the anterior-posterior and dorsal-ventral axes during Drosophila oogenesis. Curr Opin Genet Dev 9:396–404.

Vinh DB, Drubin DG. 1994. A yeast TCP-1-like protein is required for actin function in vivo. Proc Natl Acad Sci U S A 91:9116–9120.

Volberg T, Zick Y, Dror R, Sabanay I, Gilon C, Levitzki A, Geiger B. 1992. The effect of tyrosine-specific protein phosphorylation on the assembly of adherens-type junctions. EMBO J 11:1733–1742.

Wodarz A. 2002. Establishing cell polarity in development. Nat Cell Biol 4:E39–E44.

Xu T, Rubin GM. 1993. Analysis of genetic mosaics in developing and adult Drosophila tissues. Development 117:1223–1237.

Zhang Y, Kalderon D. 2000. Regulation of cell proliferation and patterning in Drosophila oogenesis by Hedgehog signaling. Development 127:2165–2176.

Zhang L, Koivisto L, Heino J, Uitto VJ. 2004. Bacterial heat shock protein 60 may increase epithelial cell migration through activation of MAP kinases and inhibition of alpha6beta4 integrin expression. Biochem Biophys Res Commun 319:1088–1095.

Developmental Dynamics